

ChemComm

Accepted Manuscript



This is an *Accepted Manuscript*, which has been through the Royal Society of Chemistry peer review process and has been accepted for publication.

Accepted Manuscripts are published online shortly after acceptance, before technical editing, formatting and proof reading. Using this free service, authors can make their results available to the community, in citable form, before we publish the edited article. We will replace this *Accepted Manuscript* with the edited and formatted *Advance Article* as soon as it is available.

You can find more information about *Accepted Manuscripts* in the [Information for Authors](#).

Please note that technical editing may introduce minor changes to the text and/or graphics, which may alter content. The journal's standard [Terms & Conditions](#) and the [Ethical guidelines](#) still apply. In no event shall the Royal Society of Chemistry be held responsible for any errors or omissions in this *Accepted Manuscript* or any consequences arising from the use of any information it contains.

Cite this: DOI: 10.1039/c0xx00000x

www.rsc.org/xxxxxx

COMMUNICATION

Detection of multiple DNA targets with a single probe using a conformation-sensitive acoustic sensor

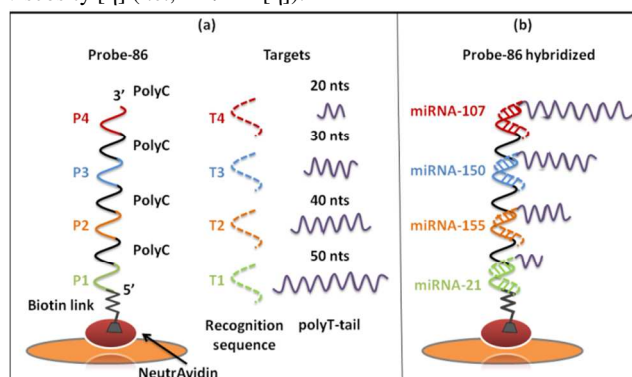
Achilleas Tsortos^a, Aristeia Grammoustianou^{a,b,‡}, Rena Lymbouridou^{a,‡}, George Papadakis^a and Electra Gizeli^{a,b}

By using an acoustic wave methodology that allows direct sensing of biomolecular conformation, we achieved the detection of multiple target DNAs with a single probe, exploiting the fact that each bound target results in a hybridized product of a different shape.

Sequence matching of nucleic acids during hybridization is the underlying molecular process behind solid phase DNA detection. A probe is first attached to a surface followed by the addition of the target analyte while the subsequent detection of the hybridized complex can be realized by means of a surface sensitive technique such as a biosensor. In the study of surface hybridization, optical and electrochemical devices are the most widely employed systems. Optical platforms based on fluorescence are highly sensitive; however, their susceptibility to fluorescent interferants present in real samples together with the need for sophisticated instrumentation make them more suitable for gene-chip lab-based analysis.¹⁻³ Optical systems based on Surface Plasmon resonance (SPR) are normally coupled to a signal amplification scheme, such as nanoparticle-conjugated systems,⁴ molecular imprinted polymers,⁵ or a hybridization-chain reaction⁶, in order to achieve the detection limits and specificity required for a diagnostically useful tool. Electrochemical biosensors are promising candidates for developing inexpensive portable platforms for on-site analysis by using direct or indirect detection schemes.^{3, 7, 8} During the last years, a new type of biosensors was presented, coupling the response of an electrochemical or optical device to a specific property of the biorecognition event, namely, a binding-induced conformational change.^{9, 10} This method exploits specific DNA probes, such as beacons,¹¹ stem loops,¹² flexible bulge-containing duplexes,¹³ hairpins¹⁴, two single stranded (ss) DNA pieces connected through PEGs,¹⁴ and clamp-like DNAs^{15, 16}, all of which undergo a significant conformational change upon target binding. In reality, both fluorescence and electrochemical sensors do not measure the

conformation of the DNA *per se*; instead, they exploit the sensors' sensitivity to the distance of a probe from another probe or the device surface, respectively, which changes as a result of target binding. Signal read-outs derived from switch- or folding-based biosensors have been shown to exhibit detection limits in the fM range.¹⁷

Acoustic biosensors are routinely used for monitoring a plethora of events such as protein binding,¹⁸ surface-fouling,¹⁹ cell-surface interactions²⁰ and DNA hybridization.^{21, 22} While originally used as a purely mass detection device, they soon evolved into a versatile tool for investigating soft matter at solvated interfaces and for obtaining structural information.²³ Recently, it was shown by our group that acoustic biosensors can sense the hydrodynamic volume of a biomolecule attached to the device surface.²⁴ Since the hydrodynamic volume is a measure of the size and shape of a molecule, it became possible to characterize and even predict DNA geometry through acoustic measurements.²⁵ The biophysical explanation is the following: single-point surface-attached DNAs are driven to oscillation by the acoustic wave. This generates a dragging force between the biomolecule and the surrounding liquid which results in energy dissipation. Theoretical modeling and experimental results showed that the ratio $\Delta D/\Delta F$ (where ΔD and ΔF are the wave energy dissipation and frequency changes, respectively) observed during molecular binding to the surface of a Quartz Crystal Microbalance (QCM) is a measure of the molecule's intrinsic viscosity $[\eta]$ (i.e., $\Delta D/\Delta F \sim [\eta]$).



Scheme 1 (a) Schematic representation of the single stranded probe and targets (i.e., recognition sequence + polyT tail) used in the assay; (b) Probe-86 hybridized to 4 targets.

^aIMBB, FORTH, 100 N. Plastira str., Heraklion, Crete, 70013, Greece. Fax: 30-2810391101; Tel: 30-2810394373

^bDept. of Biology, University of Crete, Vassilika Vouton, Heraklion Crete, 71110, Greece. Fax: 30-2810394408; Tel: 30-2810-394093

*E-mail: gizeli@imbb.forth.gr; atsortos@imbb.forth.gr

[‡]Equally contributing authors

† Electronic Supplementary Information (ESI) available

The latter is mathematically related to the geometrical features of the molecule, i.e., its conformation. The approach described above is the only reported methodology by which the acoustic ratio can be used to derive specific geometrical features of DNA, such as the bending angle, length and discriminate between spherical-, rod-, triangle-shape etc²⁴⁻²⁶. The generic nature of this novel sensing mechanism was also proven by using the Love wave platform, another liquid operating sensor based on a Surface Acoustic Wave (SAW) device^{24, 27}. It's relationship to optical methods (SPR) has also been shown²⁸.

The motivation for this work was to exploit the above approach and design a DNA detection assay where multiple targets could be acoustically detected with a single probe, simply by producing hybridization products of a different geometry each time. The simultaneous binding of two targets was also a goal, setting the challenge for designing a probe where its conformation upon binding of two targets will be distinctly different to that produced by the binding of either one of them. The design of DNA molecules of specific geometrical features is an active area of research, especially in relation to DNA structural nano-biotechnology and the production of elaborate 3-D complexes.²⁹ Here we employed a linear ssDNA probe of 86 nucleotides (nts) consisting of the following areas: four target recognition regions each one of 14nts of a different sequence placed at positions P1, P2, P3 and P4; three intermediate regions consisting of 10 poly-Cytocines (polyC); and, one surface link region comprising a biotin at the 5' end of the probe. Each ssDNA target comprised a 14nts recognition sequence complementary to one of the regions of the probe (T1 binds to P1; T2 to P2; T3 to P3 and T4 to P4) combined with a poly Thymine (polyT) tail of variable length, i.e., 20, 30, 40 and 50nts. The combination of the four target sequences with each one of the four polyT tails results in a total number of 16 analytes. For the proof of principle, we selected as targets, sequences corresponding to a particular micro RNA (miRNA21, miRNA150, miRNA155 and miRNA107). A schematic representation of the probe and targets is shown in Scheme 1a. Scheme 1b illustrates the case where all binding sites of probe-86 are hybridized to their targets; in this design, each hybridized target is linked to a polyT tail of a different size, resulting in a structure which can be paralleled to a 'tree' with the four targets forming the 'branches'.

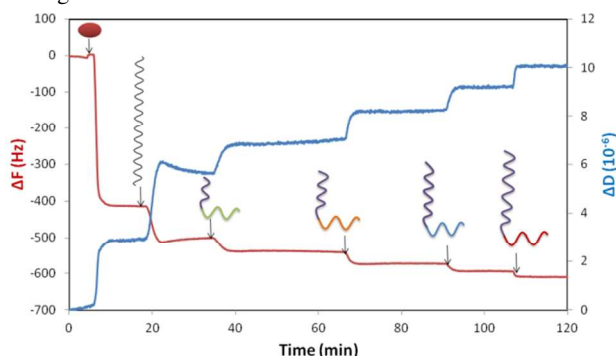


Fig. 1 Real time monitoring of dissipation and frequency changes during the addition of neutravidin (3.3 μM), probe-86 (0.2 μM), miRNA21+polyT₂₀, miRNA150+ polyT₃₀, miRNA155+polyT₄₀ and

miRNA107+polyT₅₀ (all at 4 μM); buffer (PBS) rinse followed each step. All sample volumes were 200 μl . Target miRNAs were added in amounts that do not correspond to surface saturation. Note that frequency represents raw data obtained with the QCM at 35 MHz and are not divided by the overtone number.

The experimental protocol consists of the addition of neutravidin on the QCM device surface to produce a fully covered gold substrate, followed by the binding of the biotinylated probe and sequential addition of the 4 targets. Fig. 1 depicts an experiment, where targets bearing a 20, 30, 40 or 50nts polyT tail were added to produce the hybridized product shown in Scheme 1b. The sequential addition of DNA molecules on the same surface is possible, since the acoustic ratio is independent of previous additions, order of target addition or amount of added mass. This is due to the fact that the acoustic ratio reflects intrinsic properties of the attached molecules (here conformation^{24, 26}). It is, therefore, characteristic for each DNA structure and does not change with surface coverage. This assumes that the conformation of the bound DNAs is not affected by lateral interactions with neighboring DNAs or the sensor surface, a requirement shown to be satisfied in all DNA-binding experiments including both double and single stranded molecules of various shapes and lengths.²⁴

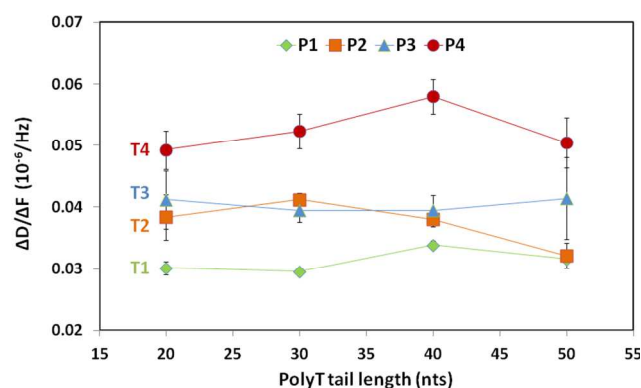


Fig. 2 Acoustic ratios of hybridized targets to probe-86, as a function of the size of the polyT tail attached to each target. Target 1 (T1: miRNA21) binds to position 1 (P1), target 2 (T2: miRNA155) to P2, target 3 (T3: miRNA150) to P3 and target 4 (T4: miRNA107) to P4. All points correspond to target-samples added at a concentration of 4 μM and in a total volume of 200 μl .

Fig. 2 gives the acoustic ratio of probe-86 after hybridization with each one of the 16 targets, as a function of the length of the attached polyT tail. This figure presents two very interesting findings. The first is related to the observation that varying the size of the branch (i.e., polyT tail) at the same position has no measurable effect on the acoustic ratio of the final hybridized product. This result implies that the emerging structures are hydrodynamically indistinguishable. Interestingly, this finding is in full agreement with data obtained in our lab showing that the intrinsic viscosity of ssDNAs in solution as well as their corresponding acoustic ratios (measured after their binding to the device-surface through biotin) vary very little for DNAs between 20 and 110nts.³⁰ An explanation of this observation would be that ssDNA molecules are not extended, as schematically depicted in Scheme 1b, but probably, adopt a shape closer to that of a rather

compact coil, of a diameter increasing with the size of the polyT tail. This shape change impacts only a marginal change on $[\eta]$.

The second finding in Fig. 2 is that a clear distinction in the measured acoustic ratio is observed when the 'branch' is placed at a different position along the probe backbone. The distance of each 'branch' with respect to the device surface is, apparently, the most crucial parameter in obtaining hybridized DNA products of different conformations. Furthermore, it appears that the exact location of the polyT tail is also crucial. 'Branches' at positions 2 and 3, i.e., 28 and 42nts away from the surface, cannot be distinguished through acoustic measurement. This according to theory²⁴ suggests again that the two constructs are too similar structurally to be hydrodynamically distinct.

We have also examined the possible effect of the probe sequence on the previous findings. For this reason the poly-C parts of the probe were replaced with random nucleotide sequences. In this case, the relative differences among the acoustic ratios of the hybridized targets were similar to the ones obtained with the original 86nts probe (see Fig. S1).

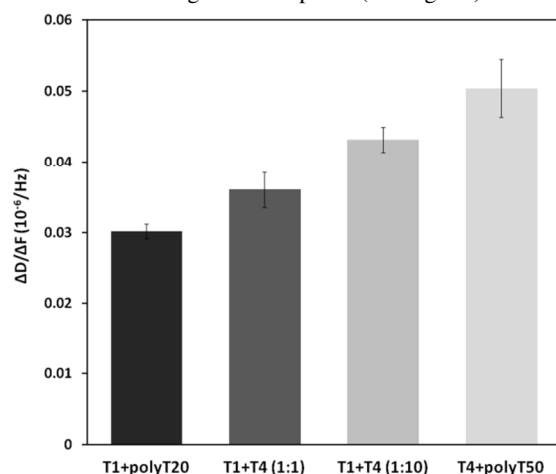


Fig. 3 Acoustic ratios corresponding to the hybridization of target T1+polyT₂₀ at P1, T4+polyT₅₀ at P4 and a combination of the two added simultaneously to the surface-immobilized probe-86 at a mole ratio of 1:1 and 1:10. Targets were added by mixing 4 μM of each one in the corresponding ratios and applied in a total volume of 200 μl.

Fig. 2 shows that an optimum discrimination is observed when DNA 'branches' are formed at P1 and P4. An interesting extension of the above work is to investigate the ability to detect simultaneously the binding of two targets. Fig. 3 gives the measured acoustic ratios during the addition of T1+polyT₂₀ at P1, T4+polyT₅₀ at P4 and a combination of the two added simultaneously to the surface-immobilized probe-86. When a mixed population of the two is used, the acoustic ratio would be expected to be in between the two values as a result of the relative number of each target on the probe, as previously demonstrated during the simultaneous binding of dsDNAs of different lengths.³¹ Fig. 3 shows that, indeed, applying the two targets in two different ratios (1:1 and 1:10) gives an acoustic ratio that lies between the ones obtained for each pure sample.

Results presented here indicate the usefulness of acoustic ratio measurements as a means of detecting and distinguishing between different DNA hybridization products by using a single probe. The underlying scientific principle is related to a new

sensing mechanism which parallels directly acoustic measurements to the conformation of surface-bound molecules. Designing probes and targets that produce distinctly different conformations upon hybridization is the necessary requirement for achieving multiple analyte detection with a good discrimination capability. Here we employ flexible polyT tails to construct 'branches' at a different position of the Probe-86 'tree'. PolyT tail was chosen instead of a random sequence to minimize non-specific interactions with the probe. In practice, such an assay could be performed in combination with an amplification step (PCR, isothermal) in order to incorporate a molecular flag such as polyT. In a recent work we showed that conformation sensing can be applied to discriminate a single nucleotide mismatch during hybridization.³² Here, the concept is extended to detect 3 different targets that are not likely to co-exist, or 2 targets simultaneously; however, the design guidelines presented can be applied to the development of a probe that could detect more than 3 hybridized targets at the same time. Such a system would be suitable for the development of multiplexed assays, such as the detection of miRNA signatures associated with several cancer types (as the ones used in this work) or other genetic diseases.^{33, 34}

The current methodology extends the concept of structure-switching electrochemical or optical systems to pure conformation-sensing acoustic biosensors.¹⁰ Through acoustic ratio measurements it is possible to detect multiple conformations as opposed to the two extreme states derived from a conformation-switching event. In addition, acoustic measurements do not necessarily rely to an enormous change in conformation, observed for example during the transition of a flexible unfolded ssDNA to a rigid well-structured double helix.⁹ In the current work we show that we can distinguish between equally flexible hybridized products as long as their hydrodynamic properties are different. Finally, the acoustic signal can also be used to detect unambiguously the recognition event, i.e., distinguish between target-specific binding as opposed to by-products or other no-specific binding by simply comparing the signal read-out (acoustic ratio) to the expected one. We envisage that the acoustic detection of the conformation of hybridized DNA molecules can form the basis of a new generation of molecular diagnosis devices for genetic biomarkers, especially given the high integration capability of SAW devices to construct simple, easy-to-operate and cost-effective Lab-on-chip platforms.³⁵

The authors would like to acknowledge financial support by the EC under FP7 (ICT Grant agreement No 317742 & Regpot/InnovCrete Grant agreement No 316223) and the General Secretariat for Research and Technology/Ministry of Education, Greece and European Regional Development Fund (Sectoral Operational Program: Competitiveness and Entrepreneurship, NSRF 2007-2013)/ European Commission (KRIPIS-BIOSYS (Project No MIS-448301) & SYNERGASIA 2011 (11SYN-5-502)).

References

1. A. Sassolas, B. D. Leca-Bouvier and L. J. Blum, *Chemical Reviews*, 2008, **108**, 109.
2. K. J. Oh, K. J. Cash and K.W. Plaxco, *Chem. Eur. J.*, 2009, **15**, 2244.
3. T. G. Drummond, M. G. Hill and J. K. Barton, *Nature Biotechnology*, 2003, **21**, 1192.
4. S. Krishnan, V. Mani, D. Wasalathanthri, C. V. Kumar and J. F. Rusling, *Angew. Chem. Int. Ed.*, 2011, **50**, 1175.
5. G-H. Yao, R-P. Liang, C-F. Huang, Y. Wang and J-D. Qiu, *Anal. Chem.*, 2013, **85**, 11944.
6. X. Li, Y. Wang, L. Wang and Q. Wei, *Chem. Comm.*, 2014, **50**, 5049.
7. J. J. Gooding, *Electroanalysis*, 2002, **14**, 1149.
8. A. Abi, and E. E. Ferapontova, *Anal. Bioanal. Chem.*, 2013, **405**, 3693.
9. A. A. Lubin, and K. W. Plaxco, *Acc. Chem. Res.*, 2010, **43**, 496.
10. K. W. Plaxco, and H. T. Soh, *Trends Biotechnol.*, 2011, **29**, 1.
11. C. Wang, Z. Zhu, Y. Song, H. Lin, C. J. Yang and W. Tan, *Chem. Comm.*, 2011, **47**, 5708.
12. R. Y. Lai, E. T. Lagally, S-H. Lee, H.T. Soh, K. W. Plaxco and A. J. Heeger, *Proc. Natl. Acad. Sci. U. S. A.*, 2006, **103**, 4017.
13. J. Chiba, A. Akaishi, R. Ikeda and M. Inouye, *Chem. Comm.*, 2010, **46**, 7563.
14. C. E. Immoos, S. J. Lee and M. W. Grinstaff, *ChemBioChem*, 2004, **5**, 1100.
15. K. W. P. A. Idili, A. Vallée-Bélisle, and F. Ricci, *ACS Nano*, 2013, **7**, 10863.
16. A. A. A. Idili, M. Vidonis, J. Feinberg-Somerson, M. Castronovo, and F. Ricci, *Anal. Chem.*, 2014, **86**, 9013.
17. Y. Xiao, A. A. Lubin, B. R. Baker, K. W. Plaxco and A. J. Heeger, *Proc. Natl. Acad. Sci. U. S. A.*, 2006, **103**, 16677.
18. T. M. A. Gronewold, *Anal. Chim. Acta*, 2007, **603**, 119.
19. S. Sheikh, D. Y. Yang, C. Blaszykowski and M. Thompson, *Chem. Comm.*, 2012, **48**, 1305.
20. M. Saitakis, and E. Gizeli, *Cell. Mol. Life Sci.*, 2012, **69**, 357.
21. C. Zerrouki, N. Fourati, R. Lucas, J. Vergnaud, J-M. Fournion, R. Zerrouki and C. Pernelle, *Biosens. Bioelectron.*, 2010, **26**, 1759.
22. T. M. A. Gronewold, A. Baumgartner, E. Quandt, and M. Famulok, *Anal. Chem.*, 2006, **78**, 4865.
23. I. Reviakine, D. Johannsmann and R. P. Richter, *Anal. Chem.*, 2011, **83**, 8838.
24. A. Tsortos, G. Papadakis, K. Mitsakakis, K. Melzak and E. Gizeli, *Biophys. J.*, 2008, **94**, 2706.
25. G. Papadakis, A. Tsortos, and E. Gizeli, *Nano Lett.*, 2010, **10**, 5093.
26. A. Tsortos, G. Papadakis, E. Gizeli, *Biosens. Bioelectron.*, 2008, **24**, 836.
27. G. Papadakis, A. Tsortos, and E. Gizeli, *Biosens. Bioelectron.*, 2009, **25**, 702.
28. F. Bender, P. Roach, A. Tsortos, G. Papadakis, M. I. Newton, G. McHale and E. Gizeli, *Meas. Sci. Technol.*, 2009, **20**, 124011.
29. M. R. Jones, N. C. Seeman, and C.A. Mirkin, *Science*, 2015, **347**.
30. A. Tsortos, G. Papadakis, and E. Gizeli, Submitted.
31. G. Papadakis, A. Tsortos, A. Kordas, I. Tiniakou, E. Morou, J. Vontas, D. Kardassis and E. Gizeli, *Sci. Rep.*, 2013, **3**.
32. G. Papadakis, A. Tsortos, F. Bender, E. E. Ferapontova and E. Gizeli, *Anal. Chem.*, 2012, **84**, 1854.
33. J. Varshney, and S. Subramanian, *Current Science*, 2014, **107**, 803.
34. J. Xia, *Cancer Mol.*, 2008, **4**, 79.
35. K. Mitsakakis, A. Tserepi, and E. Gizeli, *J. Microelectromech. S.*, 2008, **17**, 1010.